crystals

Article

Optimization and Regression Analysis of Friction Stir Processing Parameters of AA5083/Coal Composites for Marine Applications

Oritonda Muribwathoho [1,*], Velaphi Msomi [2] and Sipokazi Mabuwa [3]

[1] Mechanical and Mechatronics Department, Cape Peninsula University of Technology, Cape Town 7535, South Africa
[2] Department of Mechanical Engineering, College of Science, University of South Africa, Pretoria 0002, South Africa; msomiv@unisa.ac.za
[3] Mechanical Engineering Department, Durban University of Technology, Durban 4000, South Africa; sipokazim@dut.ac.za
* Correspondence: oritondamuribwathoho@gmail.com

Abstract: This study aimed to optimize friction stir processing parameters to enhance the mechanical properties of AA 5083/coal composites, a novel material combination with potential applications in marine environments. By systematically varying process parameters such as tilt angle, traverse speed, and rotational speed using a Taguchi experimental design, the FSP process was optimized. Signal-to-noise ratio and analysis of variance techniques were used to determine the most influential parameters on microhardness and ultimate tensile strength. A regression model was developed to predict composite behavior under these optimal conditions. This study found that a combination of 900 rpm, 60 mm/min, and a 2° tilt angle significantly improved mechanical properties. This research contributes to the advancement of FSP for producing high-performance, lightweight, and corrosion-resistant aluminum composites, particularly for marine applications.

Keywords: aluminum alloy; friction stir welding/processing; metal matrix composite; mechanical properties; Taguchi; ANOVA; S/N ratio

check for updates

Academic Editor: Hongbin Bei

Received: 27 November 2024
Revised: 19 December 2024
Accepted: 29 December 2024
Published: 30 December 2024

Citation: Muribwathoho, O.; Msomi, V.; Mabuwa, S. Optimization and Regression Analysis of Friction Stir Processing Parameters of AA5083/Coal Composites for Marine Applications. *Crystals* **2025**, *15*, 34. https://doi.org/10.3390/cryst15010034

1. Introduction

Metal matrix composites (MMCs) offer a combination of high specific strength, specific modulus, excellent high-temperature performance, and superior wear and abrasion resistance, making them highly desirable for advanced applications. Among these, aluminum-based MMCs (AMMCs) are particularly favored due to their lightweight nature and enhanced mechanical properties [1]. AA5083, a widely used aluminum alloy, stands out for its remarkable corrosion resistance, weldability, and moderate strength, making it a preferred material for marine-grade applications. However, the challenge in the field remains constantly to enhance the mechanical properties of the alloy, including tensile strength, and hardness without increasing the cost of production and affecting environmental concerns.

Over the years, various fabrication techniques have been developed to produce AMMCs, including stir casting [2–4], compo-casting [5], squeeze casting [6], spray forming [7], liquid metal infiltration [8], powder metallurgy [9], mechanical alloying, and in situ methods [10]. Each method offers unique advantages and limitations, driving ongoing research into optimizing processing techniques to achieve superior performance and efficiency. Friction stir processing (FSP) is a new technique that has been developed for joining materials for which a remelting technique is not suitable. It is an economical and environmentally friendly technique for fabricating AMMCs.

FSP does not involve conventional melting and solidification and has been used widely for improving the surface and mechanical properties of non-ferrous metals, particularly aluminum alloys with numerous types of reinforcements such as ceramics [11,12], carbon nanotubes, and particles from agricultural waste [13]. Heat is produced in FSP by the rubbing action of the tool and workpiece, contact between the pin and base metal, and dynamic recrystallization [14,15]. This heat makes the material soft and suitable for the integration of reinforcements and plastic deformation, among other processes. It was found that the process parameters used in FSP affect the quality of the composites fabricated, their microstructure, and particle distribution. Tool geometry likewise affects the material flow and heat input as indicated [16]. Second-phase particle incorporation can be achieved by way of intense material flow, but optimizing the FSP parameters is essential for improvement.

Traditional welding businesses often rely on a one-factor-at-a-time experimental approach, which is inefficient for complex processes like friction stir processing [17,18]. While mathematical iterative search techniques, problem-specific heuristics, and metaheuristics offer potential solutions [19], they are limited by their complexity, impracticality, high cost, and the requirement for a continuously differentiable objective function [20]. To address these limitations and achieve more efficient optimization, the Taguchi method provides a robust and practical alternative. By utilizing orthogonal arrays, the Taguchi method significantly reduces the number of required experiments, making it a suitable choice for industrial applications [21,22]. ANOVA determines the key parameters responsible for the variation in the output responses and evaluates the effect of one or multiple input parameters on the response [23,24].

The processing parameters in friction stir processing (FSP) play a critical role in influencing the tensile properties and microstructural characteristics of aluminum metal matrix composites (AMMCs). Understanding the interplay between these parameters and the resulting structure and properties of fabricated composites is essential for optimizing performance. Researchers have widely employed FSP in conjunction with Taguchi methods to determine optimal processing conditions for various aluminum grades and reinforcements, enabling the fabrication of high-performance metal matrix and surface composites. A review of studies focusing on the fabrication of marine-grade AMMCs reveals the use of diverse reinforcements such as ceramics (e.g., SiC, Al_2O_3), carbon nanotubes, and particles derived from agricultural waste. These materials have demonstrated significant improvements in the tribological and mechanical properties of aluminum alloys, highlighting the potential of FSP as a versatile and effective processing technique [25–33].

Singh et al. [25] studied the flow characteristics of AA5052/TiO_2/SiC hybrid surface composites employing multi-pass FSP with upward material flow. Unlike conventional downward flow, upward flow, generated by a right-handed threaded pin tool, caused plastic deformation and material movement within the stir zone. The multi-pass FSP techniques proved useful as they generated new sub-grains and improved the uniform distribution of reinforcements. The maximum microhardness of the composites achieved was 88.73 Hv after the fourth pass, and the highest tensile strength of 220.8 MPa was observed after four passes with additional improvements in the wear properties of the composites.

Bozorgmehr et al. [26] investigated the impact of traverse speed on the characteristics of microstructure, wear properties, and mechanical properties of the Al5052/ZrO_2/$ZrSiO_4$ surface hybrid fabricated by FSP at a fixed rpm 1400. The experiment was performed at test speeds of 20 mm/min, 25 mm/min, 31.5 mm/min, and 40 mm/min. The hardness, microstructure, and wear resistance of an Al5052/ZrO_2/$ZrSiO_4$ hybrid surface composite material were analyzed after effecting FSP with different traverse speeds. FSP enhanced the composite's properties because the microstructure was fine-grained and there were reinforcing particles. In this study, the slowest traverse rate of 20mm/min gave the best results of an increase in hardness of about 27.3%, and the wear resistance of the base material increased by 68.9%. This was attributed to increased heat generation and an improvement in the uniform distribution of particles, thus enhancing minimal adhesive wear.

Kaya et al. [27] examined the influence of the load (6000 N, 8000 N, and 10,000 N) and tool rotational rate (560 rpm, 710 rpm and 900 rpm) on the mechanical properties, microstructure, and wear behavior of an FSP Al5083/SiC surface composite. The study results revealed that the microhardness of the stir zone (SZ) was the highest and it was found to be about 1.4 times higher than the base material hardness.

The maximum applied forces of 8000 N, along with a critical speed of 900 rpm, offered a 38% increase in maximum hardness and an increase in wear resistance of 42%, and the ultimate tensile strength of the base material decreased by 3%.

Singhal et al. [28] fine-tuned FSP parameters for enhancing the microstructures and mechanical properties of in situ AA5083-H111/Al–Fe surficial hybrid composites. The composites under consideration were produced from Fe–40 wt% Al powder, which was subjected to mechanical alloying, and the welded samples were prepared using FSP with a reverse tool path. In a bid to minimize the number of experiments, it was necessary to utilize the Taguchi L9 orthogonal array design to collect the relevant data. The properties of FSP joined plates were investigated and quantified in terms of mechanical properties after each traverse of the FSP tool. It was noted that increasing the number of passes to a second pass led to an improvement in tensile strength from 225.8 MPa to 253.6 MPa. Microhardness also progressively increased and reached 128.3 Hv on the second pass. These improvements were attributed to optimized FSP parameters: shoulder diameters of 21 mm, traverse speed of 63 mm/min, rotational speed of 900 rpm, and tilt angle of 1.5°. Based on the fractographic analysis of the failure, it was found that the AA5083/Al–Fe composite failed in ductile mode, as expected for the system. This ductile failure mode had its contribution to the mechanical performance of the material, which was outstanding.

Venkatesh et al. [29] used the Taguchi optimization technique to study the betterment of FSW process parameters of AA6061-6% SiC composite plates by analyzing the influence of axial load, tool rotational speed, and pin profile on microhardness and UTS. The study showed that an axial load of 6 kN, a tool rotational speed of 750 rpm, and a square pin profile were effective in achieving the highest UTS. For microhardness, peak values of 6 kN, 900 rpm, and a pin profile in the form of a cylinder were identified to be optimal. ANOVA revealed that the tool profile had the most significant impact on Vickers hardness, with a percentage contribution of 53.84%, followed by tool rotational speed, with a percentage contribution of 20.16%, and axial force, with a percentage contribution of 21.32%.

Megahed et al. [30] attempted to enhance the FSP parameters of microstructure and hardness, together with the wear resistance characteristics, of AA6061/WC nanocomposite. The control factors were transverse feed, tool rotational speed, volume fraction, and number of passes of the WC nanoparticles. Detailed characterization analysis revealed that the dispersion of WC particles in the AA6061 matrix of the composite was uniform with no evidence of defect. Owing to the high strain rate and high temperature, the FSP underwent significant plastic deformation and heat, which might pin the break of coarse particles and porous holes and could promote dynamic recrystallization to generate an ultra-fine grain structure. The microhardness of the processed composite was 144 VHN, which is higher than that of the base metal by a percentage of 39.81. In all the samples, there was reduced weight loss. From the analysis of variance obtained, it was observed that the passes significantly affect microhardness by 40.1% and weight loss by 56.94% of WC volume fraction. Among all the cases studied, the maximum microhardness and wear resistance were achieved using an 1800 r.p.m. feed rate of 120 mm/min containing 6% WC and with three FSP passes.

Teo et al. [31] worked on the study of the friction stir processing parameters of recycled aluminum alloy 6063/TiO2 surface composites for enhanced tribological properties. For sample fabrication, a moderate range of process parameters was employed, and in the other case, the rotational speed was selected as 2442 rpm and the feed rate was 50 mm/min. A microhardness test was carried out for the mechanical properties of the developed material, and its friction and anti-wear properties were evaluated using a pin-on-disk tribo-tester under a starve lubrication mode. At the high setting, the research revealed enhanced surface composite mechanical properties, with a 45% enhancement in microhardness, a reduction in the friction coefficient by 39%, and a 73% reduction in the wear rate of the base materials. The study showed that TiO2 particles were well dispersed within the aluminum matrix and the average grain size was reduced, which enhanced the mechanical and wear characteristics.

Bharathikanna et al. [32] investigated the mechanical properties and corrosion behavior of friction stir processed AA6082 alloy with the addition of Cr_3C_2_particles. Tool rotation speed, axial force, and traverse speed were also analyzed in their work using Taguchi's orthogonal array and Gray Relational Analysis. Tests like tensile properties, metallographs, etc., were performed to analyze the effects of these variables. By comparing the results obtained, it was highlighted that axial force and traverse speed can significantly affect the performance of the composites. According to the above findings, it can be concluded the optimum values of parameters should be 1200 rpm, 45 mm/min, and 5 kN, as these values provide better tensile strength and surface hardness. Consequently, the investigation demonstrated that it was possible to use multi-objective optimization techniques to alter the properties of FSP AMCs.

Kumar et al. [33] fabricated Al 6082/SiC composites using FSP. SiC particles were used in different volume fractions (2%, 4%, 6%) and were dispersed in the aluminum matrix. A micrograph study depicted fine grain sizes and good interfacial adhesion of SiC-reinforced particles with the aluminum matrix. Mechanical tests proved that the ultimate tensile strength of the composites was enhanced up to 1.58-fold compared to the base material, with a hardness of 85.75 HB. The FSP process changed the Al 6082 matrix from a coarse-grained structure to a fine recrystallized grain structure with a nearly uniform distribution of SiC particles. This homogenous dispersion contributed to the improved mechanical properties and also proved the efficiency of FSP for preparing SiC-reinforced aluminum composites.

Coal, as an innovative reinforcement material, presents distinct advantages, including cost-effectiveness, abundance, and potential sustainability, setting it apart from traditional ceramic or metallic reinforcements. Despite these benefits, limited research has examined its integration into aluminum alloys, particularly for lightweight applications like those in marine environments. This study addresses this gap by optimizing the friction stir processing (FSP) parameters for AA5083/coal composites, advancing the development of cost-effective and durable materials. This study employs the Taguchi method and regression analysis to refine FSP design parameters and evaluate mechanical properties such as tensile strength and hardness. The findings are expected to demonstrate that coal can serve as a viable and economical reinforcement material, offering excellent durability for marine applications demanding long-term performance and reliability.

2. Materials and Methods

2.1. Material Selection

The base material used for this study was aluminum AA5083 plates of dimensions of 250 mm × 55 mm × 6 mm to prepare aluminum metal matrix composite materials. Based on mechanical tests, these alloys possessed an ultimate tensile strength of 311 MPa, a percentage of elongation of 58.65%, and 93.07 HV hardness. The content of the components of the AA5083 alloy is described in Table 1. The balance of this composition is important in the assessment of its material properties and the application potential of the alloy, especially concerning the friction stir processing explored in this study. Coal particles, comprising 5% of the composite's volume, were incorporated as a reinforcement material.

Table 1. The composition of AA5083-H111 in wt % [34].

BM	Cu	Cr	Cr	Fe	Mg	Mn	Si	Ti	Zn	Al
AA5083	0.02	0.05	0.05	0.16	4.03	0.69	0.15	0.02	0.01	Bal

2.2. Parameter Selection Using Taguchi

A Taguchi L9 orthogonal array was employed to systematically investigate the effects of three key FSP parameters—tool tilt angle, tool traverse speed, and tool rotational speed—on the desired response variables. MINITAB18 software was used to analyze the experimental data. Each of these parameters was used at three different levels, therefore leading to a total number of nine experimental conditions. These parameters were chosen based on prior research [35]. The experimental matrix is provided in two tables, namely, Tables 2 and 3, illustrating the precise parameter variations that were employed in the tests. This systematic method allows the different conditions of the chosen FSP parameters and their effects on the properties of the developed aluminum matrix composites to be evaluated systematically to identify the best option as informed by the results of the experiments.

Table 2. Processing factors and levels.

Level	Tilt Angle (TA) [°]	Traverse Speed (TS) [mm/min]	Rotational Speed (RS) [rpm]
1	1	30	600
2	1.75	45	900
3	2	60	1200

Table 3. Taguchi L_9 design matrix.

No of Tests	Tilt Angle [°]	Traverse Speed [mm/min]	Rotational Speed [rpm]
1.	1	30	600
2.	1.75	45	600
3.	2	60	600
4.	1.75	30	900
5.	2	45	900
6.	1	60	900
7.	2	30	1200
8.	1	45	1200
9.	1.75	60	1200

2.3. Fabrication Method

To create the aluminum metal matrix composite, two AA5083 sheets were first friction stir-welded together. Subsequently, holes of 2.5 mm diameter, 4 mm depth, and 15 mm interval along the weld line were drilled. Coal reinforcement was then inserted into these drilled holes, after which a pinless friction stir processing (FSP) tool was utilized to close them securely. Subsequently, a high-speed steel FSP tool featuring a triangular pin profile was employed to conduct the FSP pass. To detail the FSW/FSP tool, this tool has a shoulder diameter of 20 mm, a probe diameter of 7 mm, and a pin length of 5.7 mm, which enables the processing of the aluminum composite material.

3. Results and Discussions

3.1. Mechanical Properties

Following FSP, tensile and hardness specimens with orientation perpendicular to the processing direction were cut. Tensile specimens were prepared based on ASTM E-8M-04 standards [36] and tested on the Hounsfield tensile test machine. Microhardness measurements were carried out using a Vickers microhardness tester following ASTM E-384 [37] at room temperature with the help of the Innova Test Falcon 500 hardness testing machine. The tensile and microhardness specimen samples and size configuration are depicted in Figures 1 and 2 below. The tensile strength and hardness of AA5083/coal composites are represented in Table 4, highlighting the effects of different process parameters with confidence intervals (CI).

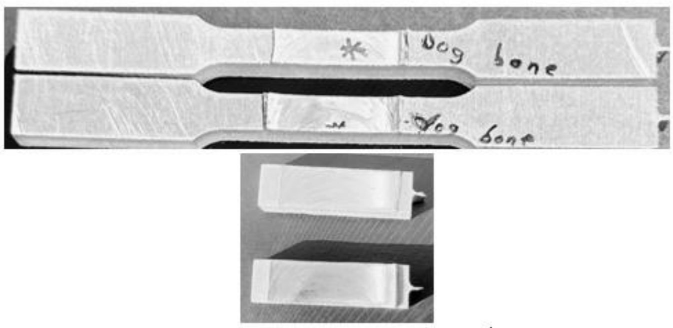

Figure 1. Samples of tensile and hardness specimens.

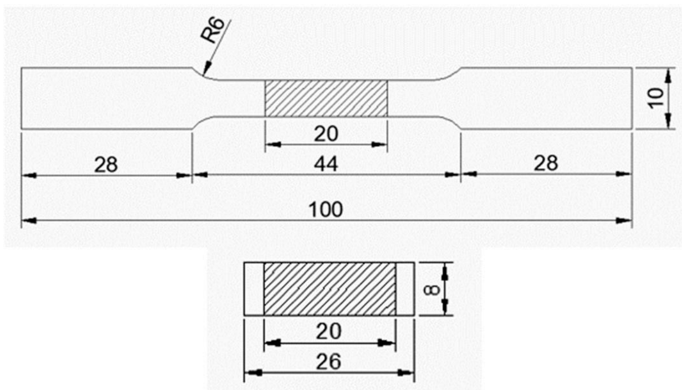

Figure 2. Tensile and hardness specimen size and configuration.

Table 4. AA5083/coal composite mechanical properties with confidence intervals.

Experiment No.	UTS (MPa)	CI for UTS (MPa)	PE (%)	CI for PE (%)	MH (HV)	CI for MH (HV)
1.	167	167 ± 5	11.9	11.9 ± 0.3	93.6	93.6 ± 0.5
2.	109	109 ± 5	7.00	7.00 ± 0.3	88.3	88.3 ± 0.5
3.	224	224 ± 5	22.4	22.4 ± 0.3	92.7	92.7 ± 0.5
4.	134	134 ± 5	12.2	12.2 ± 0.3	96.3	96.3 ± 0.5
5.	242	242 ± 5	20.7	20.7 ± 0.3	90.7	90.7 ± 0.5
6.	161	161 ± 5	21.2	21.2 ± 0.3	92.4	92.4 ± 0.5
7.	101	101 ± 5	7.60	7.60 ± 0.3	95.3	95.3 ± 0.5
8.	181	181 ± 5	12.8	12.8 ± 0.3	93.1	93.1 ± 0.5
9.	141	141± 5	9.38	9.38 ± 0.3	95.9	95.9 ± 0.5

3.1.1. Tensile Strength

The UTS of the base AA5083/coal composite was very comparable to the base AA5083 material; however, the particle reinforcement decreased the ductility of the material. The results of this study align with the literature [38–41], wherein single-pass composites recorded lower tensile strengths than the base material.

3.1.2. Hardness

Reinforcements enhance hardness, surpassing base material values. Variations due to recrystallization, grain size, particle distribution, and intermetallic particle fragmentation contribute to higher hardness [42,43]. This study's findings align with previous research [44].

3.1.3. Comparison Plots of Investigational and Regression-Predicted Values

The regression equation is adjusted with the help of taking the investigational output responses to define the correlation between the input process parameters and required mechanical properties. Equations (1)–(3) represent the regression models developed to predict the maximum tensile strength, percentage elongation, and hardness of the AA5083/coal composites.

The following equations represent the developed regression models:

$$UTS\ (MPa){:}\ 135 - 0.0428\ RS\ (rpm) + 1.38\ TS\ (mm/min) + 2.1\ TA\ (deg). \tag{1}$$

The regression equation for tensile strength indicates a negative relationship with rotational speed (*RS*) and positive relationships with traverse speed (*TS*) and tilt angle (*TA*). This aligns with physical expectations, as excessive rotational speed can lead to overheating, causing grain growth and reducing tensile strength. Conversely, higher traverse speeds promote finer grain structures and improved bonding, enhancing tensile strength. The tilt angle's positive effect is consistent with its role in optimizing material flow and ensuring adequate consolidation during *FSP*.

$$PE\ (\%){:}\ 9.9 - 0.00647\ RS\ (rpm) + 0.236\ TS\ (mm/min) - 0.53\ TA\ (deg). \tag{2}$$

The equation for percentage elongation reveals a slight reduction in elongation with increasing rotational speed and tilt angle. This is physically justifiable, as higher rotational speeds and tilt angles can introduce excessive thermal gradients and reinforce particle agglomeration, leading to reduced ductility. The positive influence of traverse speed suggests that moderate deformation rates support better distribution of reinforcements, maintaining ductility to some extent.

$$MH\ (HV): 81.65 + 0.00667\ RS\ (rpm) + 0.0183\ TS\ (mm/min) + 2.00\ TA\ (deg). \quad (3)$$

The equation for microhardness reflects a positive relationship with all parameters, with tilt angle having the most substantial influence. This supports the notion of high heat generation, where rotational and traverse speeds are high to promote the development of a fine-grained microstructure and well-distributed reinforcements that would increase the hardness of the material. Additionally, the significant effect of tilt angle highlights its critical role in achieving optimal surface contact and particle integration during FSP.

Below, we detail the alignment with physical expectations achieved by these equations.

The regression equations generally align with established theories of material behavior under FSP. The dominant role of traverse speed and tilt angle in tensile strength and microhardness is consistent with their impact on material flow and thermal dynamics. But such variations regarding physical expectations, for instance, the incremented positive slope of rotational speed on microhardness, may be due to local variation in heat input or particle distribution that the regression model has failed to capture completely.

The findings determined using the regression equations to analyze the mechanical properties of AA5083/coal composites are shown in Table 5. Figure 3 displays the relative UTS, PE, and MH obtained from experiment and regression equations predictions.

Table 5. Regression-predicted values with % errors.

Experiment No.	*UTS* (MPa)	Fits	Error (%)	*PE* (%)	Fits	Error (%)	*MH* (HV)	Fits	Error (%)
1.	167	153.2	8.270	11.9	12.6	6.030	93.6	88.2	5.77
2.	109	175.4	60.92	7.00	15.7	125.2	88.3	89.9	1.89
3.	224	196.6	12.25	22.4	19.2	14.38	92.7	90.7	2.11
4.	134	141.9	5.900	12.2	10.3	15.74	96.3	91.7	4.78
5.	242	163.8	32.60	20.7	13.7	33.85	90.7	92.5	1.95
6.	161	181.7	12.87	21.2	17.8	16.22	92.4	90.8	1.79
7.	101	129.6	28.30	7.60	8.21	7.970	95.3	942	1.16
8.	181	148.2	18.12	12.8	12.8	4.100	93.1	92.5	0.67
9.	141	170.4	20.87	9.38	15.4	64.47	95.9	94.2	1.73

Confidence intervals: *CI* for *UTS* (MPa) = ±5 *CI* for *PE* (%) = ±0.3 *CI* for *MH* (HV) = ±0.5.

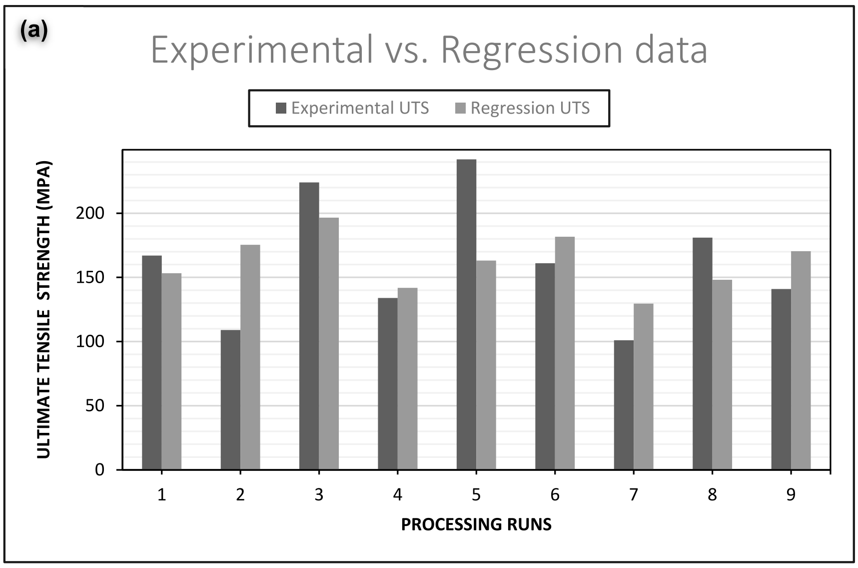

Figure 3. *Cont*.

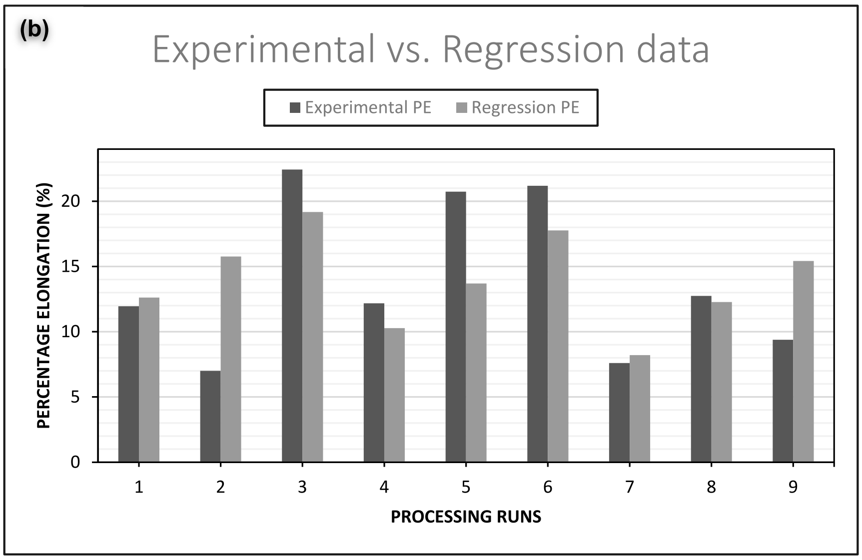

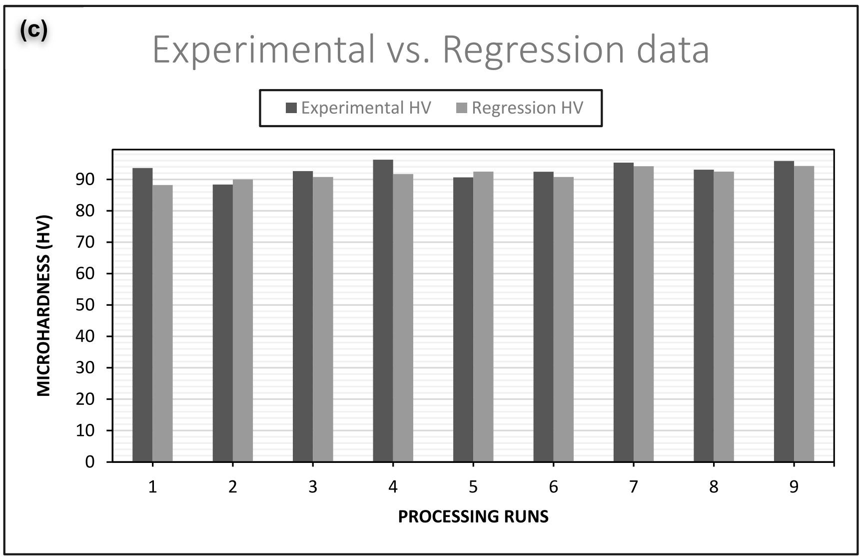

Figure 3. Experimental and regression predicted values: (**a**) ultimate tensile strength; (**b**) percentage elongation; and (**c**) microhardness.

3.1.4. Microstructural Analysis

Figure 4 displays the optical microstructures of the composites evaluated under varying friction stir processing (FSP) parameters. Figure 4a–c illustrate the microstructure of the AA5083/coal composite at rotational speeds of 600 rpm and traverse speeds of 30 mm/min, 45 mm/min, and 60 mm/min, with corresponding tilt angles of 1°, 1.75°, and 2°, respectively. Similarly, Figure 4d–f present the microstructures at 900 rpm, with tilt angles of 1.75°, 2°, and 1°, paired with traverse speeds of 30 mm/min, 45 mm/min, and 60 mm/min, respectively. Lastly, Figure 4g–i detail the microstructure at 1200 rpm, where the tilt angles and traverse speeds are set at 2° and 30 mm/min, 1° and 45 mm/min, and 1.75° and 60 mm/min, respectively.

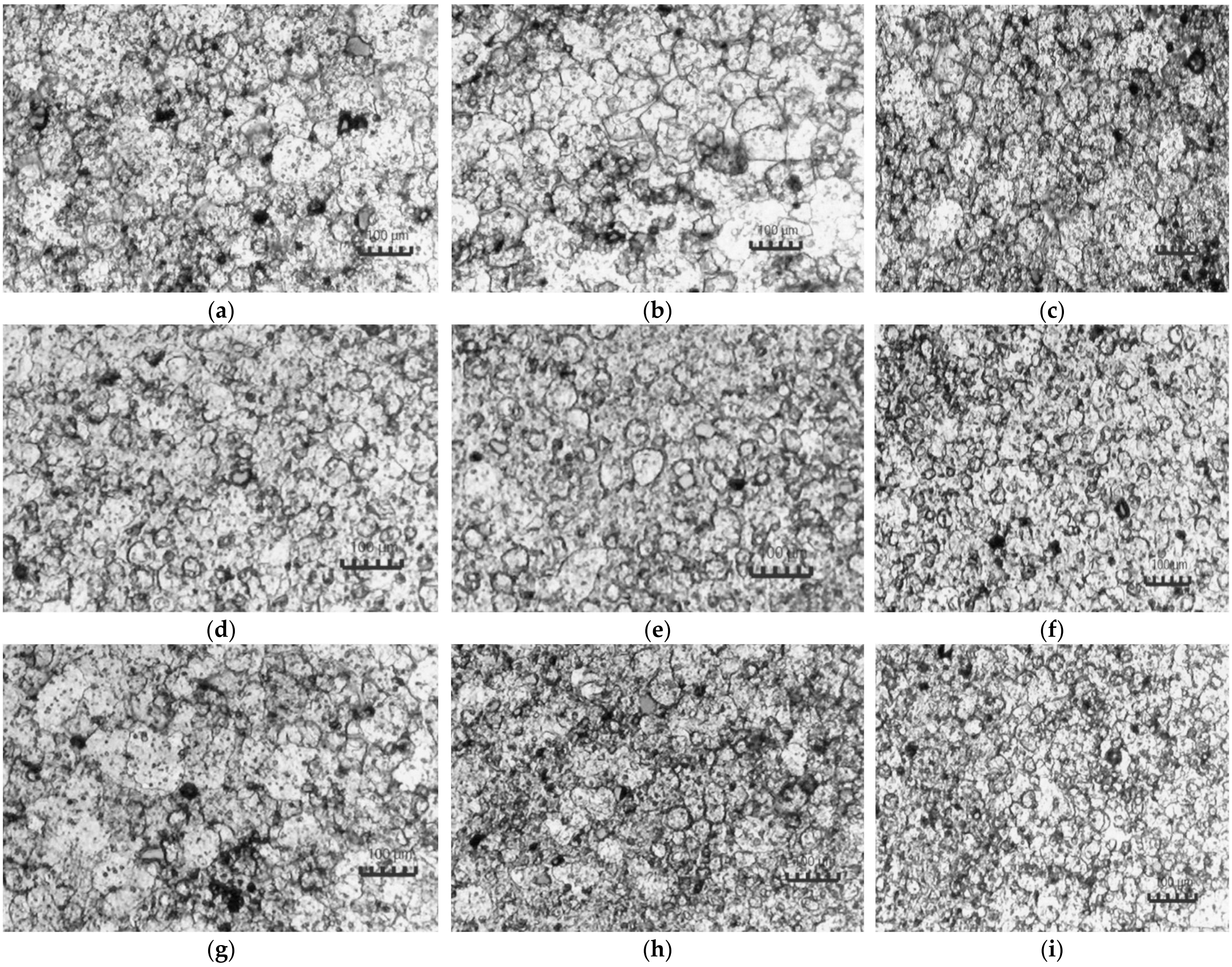

Figure 4. Optical microstructures of AA5083/coal composites captured at 20× 100 μm magnification, showing the effects of varying FSP parameters. (**a**–**c**) Microstructures at 600 rpm with traverse speeds of 30 mm/min, 45 mm/min, and 60 mm/min, and tilt angles of 1°, 1.75°, and 2°, respectively. (**d**–**f**) Microstructures at 900 rpm with traverse speeds of 30 mm/min, 45 mm/min, and 60 mm/min, and tilt angles of 1.75°, 2°, and 1°, respectively. (**g**–**i**) Microstructures at 1200 rpm with traverse speeds of 30 mm/min, 45 mm/min, and 60 mm/min, and tilt angles of 2°, 1°, and 1.75°, respectively.

The microstructural analysis provides crucial insights into the dispersion of coal reinforcement particles within the AA5083 matrix, highlighting the influence of varying FSP parameters on particle distribution and bonding. The images indicate that while coal particles are present within the stir zone, the percentage of bonded particles appears low, potentially due to limited material flow during processing [45–49]. These findings align with observations in [50–52], which noted that non-uniform particle dispersion significantly impacts the failure behavior and plastic deformation of metal-based composites.

This uneven distribution and incomplete bonding between the coal reinforcement and the matrix adversely affect mechanical properties, including tensile strength and ductility [50,53]. These results underscore the critical role of processing conditions in optimizing particle dispersion and improving the overall composite performance.

3.2. Signal-to-Noise Ratio Analysis

In order to compare the means of the responses obtained for varying levels of speed, feed, and tilt angle and find out the significance of speed, feed, and tilt angle on hardness and tensile strength, the data were analyzed by using MINITAB18 software. For this, the following steps were taken: The means and signal/noise ratio were calculated. The goal was to maximize hardness and tensile strength, so "the-larger-the-better" criteria were used for signal-to-noise ratio calculations. For optimization, S/N ratios are used instead of mean values to evaluate response characteristics. The choice of S/N ratio depends on the desired outcome. Since higher values of microhardness and ultimate tensile strength are desirable, a "the-higher-the-better" quality characteristic is applicable. This corresponds to a higher S/N ratio, indicating optimal process parameter levels.

"The-larger-the-better" signal-to-noise ratio can be calculated using the following formula [54–57]:

$$\frac{S}{N} = -10\log\left(\frac{1}{n}\sum_{i-1}^{3}\frac{1}{y^2}\right) \tag{4}$$

where n = the number of experimental repetitions and y = the re-response factor at the i-th level. The S/N ratio for parameter combinations for AA5083/coal composite based on the experimental test result is also presented in Table 6 and Figure 5.

Table 6. S/N ratio on ultimate tensile strength, percentage elongation, and hardness.

Experiment No.	*UTS* (MPa)	*S/N* Ratio For *UTS*	*PE* (%)	*S/N* Ratio For *PE*	*MH* (HV)	*S/N* Ratio For *HV*
1.	167	44.45	11.9	21.55	93.6	38.66
2.	109	40.745	7.00	16.90	88.3	38.92
3.	224	47.00	22.4	27.02	92.7	39.34
4.	134	42.54	12.2	21.71	96.3	39.67
5.	242	47.68	20.7	26.33	90.7	39.15
6.	161	44.14	21.2	26.52	92.4	39.34
7.	101	40.09	7.60	17.62	95.3	39.42
8.	181	45.15	12.8	22.11	93.1	39.38
9.	141	42.98	9.38	19.44	95.9	39.28

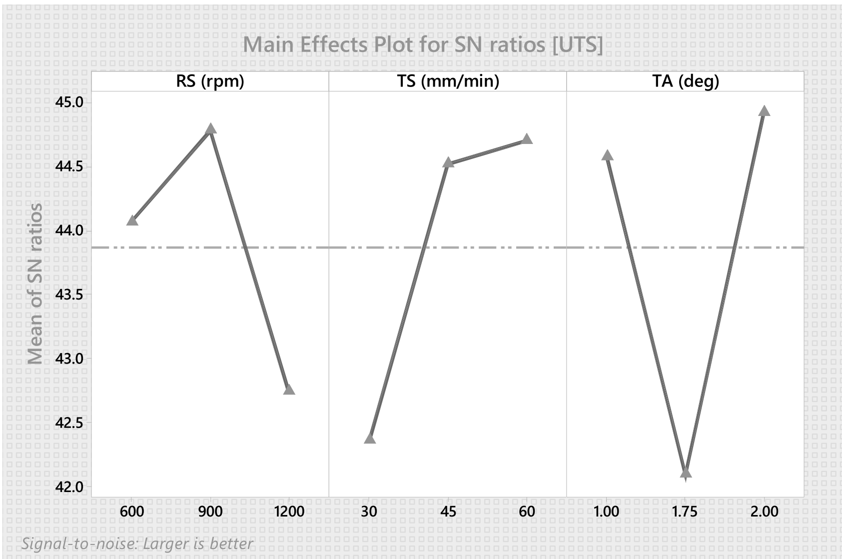

(**a**)

Figure 5. *Cont.*

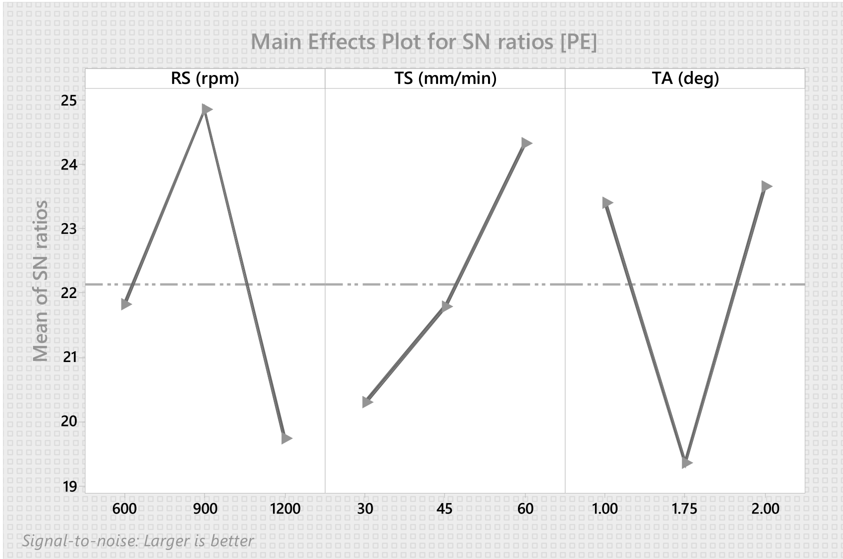

(**b**)

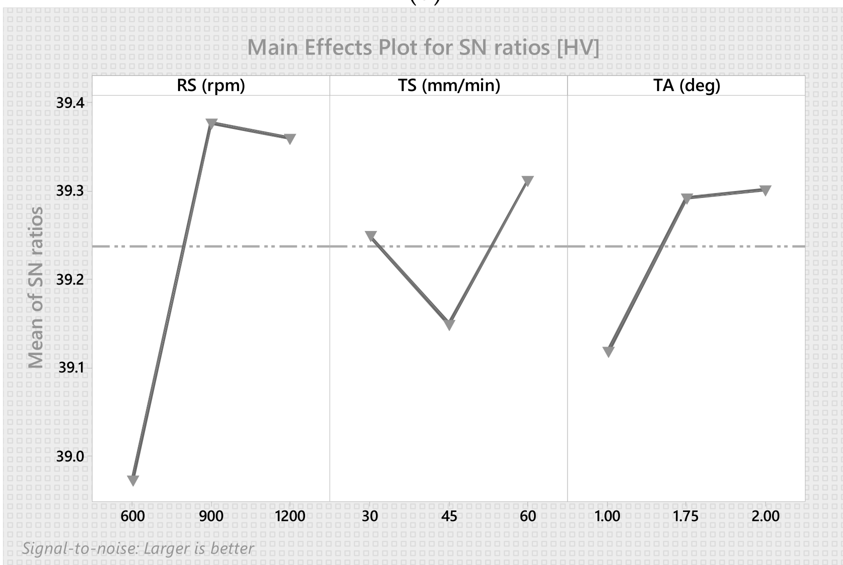

(**c**)

Figure 5. AA5083/coal composite *SN* ratio and mean plot: (**a**) *UTS*; (**b**) PE; (**c**) *HV*.

For the AA5083/coal composite, the increases in ultimate tensile strength, percentage elongation, and microhardness by tilt angle at level three, traverse speed at level three, and rotary speed at level two are shown in Figure 5. In the experiment, it was found that the best parameters were achieved at a tilt angle of 2 degrees, a traverse speed of 60 mm/min, and a rotational speed of 900 rpm. Earlier works [56,57] have used a larger-is-better approach to optimize the mechanical characteristics of metal matrix composites.

Ranking of Contributing Factors and Determining Optimum Conditions

The *S*/*N* ratios and mean responses of *UTS*, *PE*, and *HV* are depicted in Tables 7–9. The results in Table 7 also illustrate that tilt angle has the highest impact on UTS at rank 1, followed by traverse speed at rank 2 and rotational speed at rank 3. Rating analysis of the extent of effects provided in Table 8 shows that percentage elongation is most influenced by rotational speed at rank 1, followed by tilt angle at rank 2 and then traverse speed at rank 3. Finally, the values ranking the input parameters with respect to microhardness are presented in Table 9. Among those, rotational speed is most important, tilt angle is the second most important, and traverse speed is the least important parameter. From the main effects response results, it is clear that the best values for process parameters that yield the highest UTS, PE, and HV are rpm 900, feed rate 60mm/min, and angle 2°, as discussed in Section 3.2.

Table 7. Main effect response table for ultimate tensile strength.

Level	*S/N* Ratio Response			Mean Response		
	Tilt Angle (°)	Traverse Speed (mm/min)	Rotational Speed (rpm)	Tilt Angle (°)	Traverse Speed (mm/min)	Rotational Speed (rpm)
1	44.58	42.36	44.07	169.7	134.0	166.7
2	42.09	44.53	44.78	128.0	177.3	179.0
3	44.92	44.71	42.74	189.0	175.3	141.0
Delta	2.83	2.35	2.04	61.0	43.3	38.0
Rank	1	2	3	1	2	3

Table 8. Main effect response table for S/N ratio of parameters on percentage elongation.

Level	*S/N* ratio Response			Mean Response		
	Tilt Angle (°)	Traverse Speed (mm/min)	Rotational Speed (rpm)	Tilt Angle (°)	Traverse Speed (mm/min)	Rotational Speed (rpm)
1	23.39	20.29	21.82	15.29	10.58	13.79
2	19.35	21.78	24.85	9.520	13.49	18.03
3	23.65	24.33	19.72	16.92	17.66	9.910
Delta	4.30	4.03	5.13	7.400	7.087	8.120
Rank	2	3	1	2	3	1

Table 9. Main effect response table for S/N ratio of parameters on microhardness.

Level	*S/N* Ratio Response			Mean Response		
	Tilt Angle (°)	Traverse Speed (mm/min)	Rotational Speed (rpm)	Tilt Angle (°)	Traverse Speed (mm/min)	Rotational Speed (rpm)
1	39.12	39.25	38.97	90.41	91.84	88.90
2	39.29	39.15	39.38	92.23	90.69	93.12
3	39.31	39.31	39.36	92.28	92.39	92.90
Delta	0.18	0.16	0.40	1.87	1.69	4.22
Rank	2	3	1	2	3	1

3.3. Analysis of Variance

In the evaluation of process parameters, ANOVA was applied to identify the statistical significance of the findings. A frequency test was used in statistics to analyze the parameter effects that define the quality of properties [58]. From the analysis conducted below, the parameter contribution to the output response in terms of percentile and F-value (probability distribution) was established. Tables 10 and 11 show the results of analysis of variance for the signal-to-noise ratio and mean of ultimate tensile strength, percentage elongation, and hardness. Based on the analysis of variance results, none of the factors (TA, TS, and RS) were found to have a statistically significant impact on any of the response variables (UTS, PE, and HV) at the 0.05 significance level. This indicates that the experimental design may not have been effective in identifying significant factors or that the chosen factors do not have a strong influence on the responses. Further analysis, such as examining interaction effects or refining the experimental design, may be necessary to gain more insights.

Table 10. Factor contribution to the variation in S/N ratio.

Source	Degree of Freedom (DF)	Seq SS	Adj SS	Adj MS	% Contribution	F-Value	*p*-Value
For UTS							
TA (°)	2	14.33	14.33	7.165	**27.05**	0.65	0.605
TS (mm/min)	2	10.23	10.23	5.116	**19.31**	0.47	0.682
RS (rpm)	2	6.451	6.451	3.226	**12.18**	0.29	0.773
Error	2	21.97	21.97	10.98	**41.47**		
Total	8	52.98					
For PE							
TA (°)	2	34.89	34.89	17.45	**30.03**	2.12	0.320
TS (mm/min)	2	24.97	24.97	12.49	**21.89**	1.52	0.397
RS (rpm)	2	39.93	39.93	19.96	**34.36**	2.43	0.292
Error	2	16.44	16.44	8.221	**14.15**		
Total	8	116.2					
For HV							
TA (°)	2	0.064	0.064	0.032	**9.169**	0.23	0.815
TS (mm/min)	2	0.040	0.040	0.020	**5.731**	0.14	0.874
RS (rpm)	2	0.313	0.313	0.157	**44.84**	1.12	0.472
Error	2	0.280	0.280	0.140	40.11		
Total	8	0.698					

Table 11. Factor contribution to the variation in means.

Source	Degree of Freedom (DF)	Seq SS	Adj SS	Adj MS	% Contribution	F-Value	*p*-Value
For UTS							
TA (°)	2	5831	5831	2915	31.71	0.87	0.535
TS (mm/min)	2	3590	3590	1795	19.53	0.54	0.651
RS (rpm)	2	2255	2255	1127	12.27	0.34	0.748
Error	2	6710	6710	3355	36.49		
Total	8	18386					
For PE							
TA (°)	2	90.74	90.74	45.37	31.48	4.05	0.198
TS (mm/min)	2	76.12	76.12	38.06	26.41	3.40	0.227
RS (rpm)	2	98.96	98.96	49.48	34.33	4.42	0.185
Error	2	22.40	22.40	11.20	7.772		
Total	8	288.2					
For HV							
TA (°)	2	6.799	6.799	3.400	8.948	0.22	0.820
TS (mm/min)	2	4.477	4.477	2.239	5.892	0.14	0.873
RS (rpm)	2	33.83	33.83	16.91	44.52	1.10	0.477
Error	2	30.88	30.88	15.44	40.64		
Total	8	75.98					

Percentage of Contributions

Figure 6 displays the percentage contribution based on ANOVA. The ANOVA of the S/N ratio for UTS, PE, and HV reveals that tilt angle significantly impacts the output response for ultimate tensile strength, with a percentage of 27.05%. Elongation and hardness also show strong dependency on tool rotational speed, at 34.37% and 44.84%, respectively. The frequency value agrees with the contribution percentage and the ranking in the table. The results support the importance of tool rotational speed in the output response. The tilt angle's impact on tensile strength is due to its control over material flow and tool penetration, which are essential for defect prevention and bonding [59]. Rotational speed significantly influences microhardness, emphasizing the significance of heat generation in grain refinement and particle distribution [60–62].

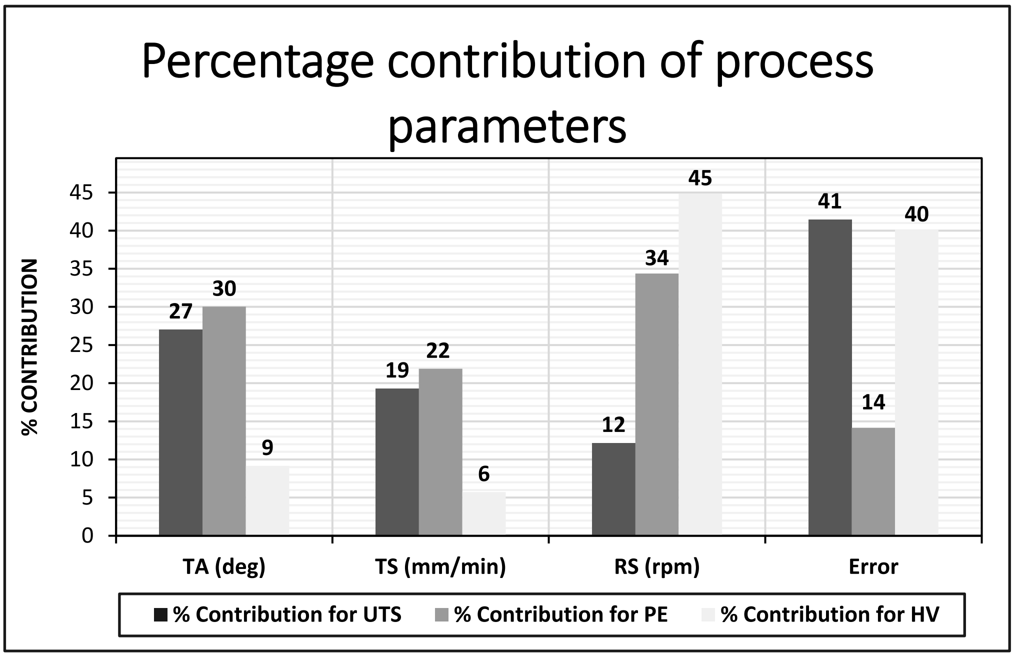

Figure 6. Percentage contribution of process parameters for UTS, PE, and HV.

3.4. Confirmation Test

Additional experiments were conducted using the identified optimal settings to validate the optimized process parameters. The tool rotational speed, traverse speed, and tilt angle were set to 900 rpm, 60 mm/min, and 2 degrees [63]. Three confirmation tests were conducted on AA5083/coal composites. The average UTS was found to be 244.7 MPa. The average hardness was determined to be 91.42. These confirmation tests demonstrated the effectiveness of the optimized parameters in enhancing the mechanical properties of the composites, reinforcing the findings from the initial experimental phase.

4. Conclusions

This study successfully optimized the fabrication of AMMCs using friction stir processing and the Taguchi L9 factorial method. This study effectively developed a surface composite by employing AA5083 as the matrix material and coal as the reinforcement. The Taguchi method was employed to identify the optimal process parameters for maximizing both tensile strength and hardness in the AA5083/coal composite. The Taguchi technique allowed us to draw the following conclusions:

- The experimental tensile strength of the AA5083/coal composite reached a maximum of 242 MPa, which is comparable to the 311 MPa ultimate tensile strength of the base AA5083 material. Although the composite exhibited similar mechanical properties to the base material, its ductility was reduced due to the presence of reinforcing coal particles.
- The experimental microhardness of the AA5083/coal composite reached a maximum of 96.3 HV, which is higher than the 93.1 HV hardness of the base material AA5083. The incorporation of reinforcements enhanced the hardness of the composite, surpassing the base material values. These parameters include recrystallization, grain refinement, particle distribution, and intermetallic particle fracture.

- The extent to which tool rotation, traverse speed, and tool tilt influenced the tensile strength, elongation, and hardness of the AA5083/coal composite joints was found to be highest at 900 rpm, 60 mm/min, and 2 degrees, in that order. Specific values for tilt angle, traverse speed, and rotational speed set at level 3 and level 2 resulted in optimal mechanical properties for these features.
- The ANOVA results revealed that tilt angle was the most influential factor influencing ultimate tensile strength, contributing 27.047% to the overall variance. Traverse speed and rotational speed followed, accounting for 19.307% and 12.176%, respectively. For percentage elongation, rotational speed emerged as the most significant factor, contributing 34.368% to the variance. Tilt angle and traverse speed had contributions of 30.025% and 21.888%, respectively. Finally, rotational speed was again identified as the most influential factor for microhardness, contributing 44.842% to the variance. Tilt angle and traverse speed followed, with contributions of 9.1691% and 5.7306%, respectively.
- Despite this, the regression models used give useful predictive estimates, and their validity is constrained by the design of the experiment and the ranges of the parameters used. Further analysis incorporating interaction terms or advanced regression techniques (e.g., response surface methodology) could offer a more nuanced understanding of the complex interdependencies between FSP parameters and mechanical properties.

5. Limitations

Although this study did not directly assess corrosion resistance, AA5083 is well-known for its exceptional corrosion performance in marine environments. Future research will focus on evaluating the effect of coal reinforcement on the alloy's corrosion resistance and its durability under simulated marine conditions.

6. Scientific Contributions

The authors' scientific contribution lies in the innovative use of coal particles as a reinforcement material for AA5083 aluminum matrix composites produced through friction stir processing (FSP). This study uniquely integrates the Taguchi method and regression analysis to systematically optimize FSP parameters—rotational speed, traverse speed, and tilt angle—and examine their impact on mechanical properties such as tensile strength, hardness, and ductility.

In contrast to prior research, which primarily focuses on conventional reinforcements like ceramics or carbon-based materials, this study explores the potential of coal as a plentiful, cost-effective, and environmentally sustainable alternative. The findings provide valuable insights into the viability of incorporating coal particles into aluminum alloys, particularly for marine applications, where corrosion resistance and mechanical performance are crucial. Moreover, the inclusion of confirmation tests enhances the reliability of the optimized parameters, establishing a robust framework for future research on unconventional reinforcement materials.

Author Contributions: Conceptualization, V.M.; methodology, S.M.; software, O.M.; validation, O.M., V.M., and S.M.; formal analysis, S.M.; investigation, O.M.; resources, V.M.; data curation, S.M. and OM.; writing—original draft, O.M.; writing—review and editing, S.M. and V.M.; visualization, O.M.; supervision, V.M. and S.M.; project administration, V.M. All authors have read and agreed to the published version of the manuscript.

Funding: This research received no external funding.

Data Availability Statement: Data are contained within this article.

Acknowledgments: The authors would like to thank the Cape Peninsula University of Technology for granting the authors a chance to use the equipment required in this study as much as possible.

Conflicts of Interest: The authors declare that they have no conflicts of interest.

References

1. Thandalam, S.K.; Ramanathan, S.; Sundarrajan, S. Synthesis, microstructural and mechanical properties of ex-situ zircon particles (ZrSiO4) reinforced Metal Matrix Composites (MMCs): A review. *J. Mater. Res. Technol.* **2015**, *4*, 333–347. [CrossRef]
2. Kumar, T.S.; Subramanian, R.; Shalini, S.; Angelo, P.C. Microstructure, mechanical properties and corrosion behaviour of Al–Si–Mg alloy matrix/zircon and alumina hybrid composite. *Forsch. Im Ingenieurwesen* **2015**, *79*, 123–130. [CrossRef]
3. Kumar, T.S.; Subramanian, R.; Shalini, S.; Anburaj, J.; Angelo, P.C. Synthesis, microstructure and mechanical properties of Al-Si-Mg alloy hybrid (zircon+ alumina) composite. *Indian J. Eng. Mater. Sci.* **2016**, *23*, 20–26.
4. Kumar, T.S.; Subramanian, R.; Shalini, S.; Angelo, P.C. Age hardening behaviour of Al-Si-Mg alloy matrix/zircon and alumina hybrid composite. *J. Sci. Ind. Res.* **2016**, *75*, 89–94.
5. Sharma, S.C.; Girish, B.M.; Somashekar, D.R.; Satish, B.M.; Kamath, R. Sliding wear behaviour of zircon particles reinforced ZA-27 alloy composite materials. *Wear* **1999**, *224*, 89–94. [CrossRef]
6. Ejiofo, J.U.; Okorie, B.A.; Reddy, R.G. Powder processing and properties of zircon-reinforced Al-13.5 Si-2.5 Mg alloy composites. *J. Mater. Eng. Perform.* **1997**, *6*, 326–334. [CrossRef]
7. Abdizadeh, H.; Ashuri, M.; Moghadam, P.T.; Nouribahadory, A.; Baharvandi, H.R. Improvement in physical and mechanical properties of aluminum/zircon composites fabricated by powder metallurgy method. *Mater. Des.* **2011**, *32*, 4417–4423. [CrossRef]
8. Kaur, K.; Pandey, O.P. Microstructural characteristics of spray formed zircon sand reinforced LM13 composite. *J. Alloys Compd.* **2010**, *503*, 410–415. [CrossRef]
9. Weissgaerber, T.; Kieback, B. Dispersion strengthened materials obtained by mechanical alloying-an overview. *Mater. Sci. Forum* **2000**, *34*, 275–283. [CrossRef]
10. Reddy, B.S.; Das, K.; Das, S. A review on the synthesis of in situ aluminum-based composites by thermal, mechanical and mechanical–thermal activation of chemical reactions. *J. Mater. Sci.* **2007**, *42*, 9366–9378. [CrossRef]
11. Salih, O.S.; Ou, H.; Wei, X.; Sun, W. Microstructure and mechanical properties of friction stir welded AA6092/SiC metal matrix composite. *Mater. Sci. Eng. A* **2019**, *742*, 78–88. [CrossRef]
12. Abioye, T.E.; Zuhailawati, H.; Anasyida, A.S.; Yahaya, S.A.; Dhindaw, B.K. Investigation of the microstructure, mechanical and wear properties of AA6061-T6 friction stir weldments with different particulate reinforcements addition. *J. Mater. Res. Technol.* **2019**, *8*, 3917–3928. [CrossRef]
13. Hussain, Z.; Halmy, M.N.; Almanar, I.P.; Dhindaw, B.K. Friction stir processed of 6061-T6 aluminum alloy reinforced with silica from rice husk ash. *Adv. Mater. Res.* **2014**, *1024*, 227–230. [CrossRef]
14. Mr, P.S.; Badheka, V. An experimental investigation of temperature distribution and joint properties of Al 7075 T651 friction stir welded aluminium alloys. *Procedia Technol.* **2016**, *23*, 543–550.
15. Patel, V.V.; Badheka, V.J.; Kumar, A. Influence of pin profile on the tool plunge stage in friction stir processing of Al–Zn–Mg–Cu alloy. *Trans. Indian Inst. Met.* **2017**, *70*, 1151–1158. [CrossRef]
16. Elangovan, K.; Balasubramanian, V. Influences of pin profile and rotational speed of the tool on the formation of friction stir processing zone in AA2219 aluminium alloy. *Mater. Sci. Eng. A* **2007**, *459*, 7–18. [CrossRef]
17. Pawar, S.P.; Shete, M.T. Optimization of friction stir welding process parameter using taguchi method and response surface methodology: A review. *Int. J. Res. Eng. Technol.* **2013**, *2*, 551–554.
18. Lakshminarayanan, A.K.; Balasubramanian, V. Process parameters optimization for friction stir welding of RDE-40 aluminium alloy using Taguchi technique. *Trans. Nonferrous Met. Soc. China* **2008**, *18*, 548–554. [CrossRef]
19. Mukherjee, I.; Ray, P.K. A review of optimization techniques in metal cutting processes. *Comput. Ind. Eng.* **2006**, *50*, 15–34. [CrossRef]
20. Markos, S.; Viharos, Z.J.; Monostori, L. Quality-oriented, comprehensive modeling of machining processes. In Proceedings of the Sixth ISMQC IMEKO Symposium on Metrology for Quality Control in Production, Vienna, Austria, 8–10 September 1998; pp. 67–74.
21. Montgomery, D.C. *Design and Analysis of Experiments*; John Wiley & Sons: Hoboken, NJ, USA, 2017.
22. Kowalczyk, M. Application of Taguchi and ANOVA methods in the selection of process parameters for surface roughness in precision turning of titanium. *Adv. Manuf. Sci. Technol.* **2014**, *2*. [CrossRef]
23. Ross, P.J. Taguchi techniques for quality engineering: Loss function, orthogonal experiments, parameter and tolerance design. *Natl. Acad. Sci. Eng. Med.* **1988**.
24. Santha, D.R.; Ramanaiah, N. Process Parameters Optimization for Producing AA6061/TiB Composites by Friction Stir Processing. *Stroj. Časopis-J. Mech. Eng.* **2017**, *67*, 101–118. [CrossRef]

25. Singh, D.; Sarvaiya, J. Development of AA5052/TiO2/SiC hybrid surface composites using upward material flow through multipass friction stir processing. *J. Adhes. Sci. Technol.* **2023**, *37*, 3335–3357. [CrossRef]
26. Bozorgmehr, M.; Heidari, A.; Amini, K.; Loh Mousavi, M.; Gharavi, F. The effect of traverse speed in friction stir process on the microstructure, mechanical properties and wear behavior Al5052/ZrO2/ZrSiO4 surface hybrid composite. *J. Weld. Sci. Technol. Iran* **2024**, *9*, 1–4.
27. Kaya, N.; Çetinkaya, C.; Karakoç, H.; Ada, H. Effect of process parameters of Al5083/SiC surface composites fabricated by FSP on microstructure, mechanical properties and wear behaviors. *Mater. Chem. Phys.* **2024**, *315*, 128991. [CrossRef]
28. Singhal, V.; Jain, V.K.; Raman, R.S.; Patharia, D.; Mittal, V.; Mishra, S.; Kumar, H. Optimization of friction stir processing parameters for improving structural and mechanical properties in in situ AA5083-H111/Al–Fe composites. *Proc. Inst. Mech. Eng. Part C J. Mech. Eng. Sci.* **2024**, *238*, 4477–4490. [CrossRef]
29. Venkatesh, B.N.; Hebbal, U.; Siddappa, P.N.; Kousik, S.; Nagaraja, T.K. Optimization of FSW parameters of AA6061-6 wt.% SiC composite plates. *Manuf. Rev.* **2022**, *9*, 34.
30. Megahed, A.A.; Mohamed, M.A.; Abdel Hamid, M.; Zoalfakar, S.H. Microstructure, hardness, and wear properties of AA6061/WC nanocomposite fabricated by friction stir processing. *Proc. Inst. Mech. Eng. Part C J. Mech. Eng. Sci.* **2022**, *236*, 9148–9156. [CrossRef]
31. Teo, G.S.; Liew, K.W.; Kok, C.K. A study on friction stir processing parameters of recycled AA 6063/TiO2 surface composites for better tribological performance. *Metals* **2022**, *12*, 973. [CrossRef]
32. Bharathikanna, R.; Elatharasan, G. Microstructure, Mechanical and Corrosion Behavior of Friction Stir Processed AA6082 with Cr 3 C 2 Particles. *Soldag. Inspeção* **2022**, *27*, e2723. [CrossRef]
33. Kumar, N.; Gupta, P.; Singh, R.K. Fabrication of Al 6082/SiC composite using friction stir processing. *J. Inst. Eng. Ser. D* **2023**, *104*, 603–608. [CrossRef]
34. Zass, K.; Mabuwa, S.; Msomi, V. Introduction of Coal Reinforcing Particles on the Dissimilar FSW AA608/AA5083 Joint via Friction Stir Processing. *Metals* **2023**, *13*, 1981. [CrossRef]
35. Kosaraju, S.; Aziz, M.A.; Yadav, V.P.; Shiva, B.; Kolli, M.; Cheepu, M. Taguchi optimization of friction stir process parameters for enhancing joint strength of AA8011 reinforced with SiC nano particles. *Int. J. Interact. Des. Manuf.* **2024**, 1–12. [CrossRef]
36. *ASTM E8M-04*; Standard Test Methods for Tension Testing of Metallic Materials. ASTM International: West Conshohocken, PA, USA, 2004; pp. 1–24.
37. *ASTM E384-11*; Standard Test Method for Microindentation Hardness of Materials. ASTM International: West Conshohocken, PA, USA, 2011; pp. 1–24.
38. Ayvaz, S.I.; Arslan, D.; Ayvaz, M. Investigation of mechanical and tribological behavior of SiC and B4C reinforced Al-Zn-Mg-Si-Cu alloy matrix surface composites fabricated via friction stir processing. *Mater. Today Commun.* **2022**, *31*, 103419. [CrossRef]
39. Yuvaraj, N.; Aravindan, S. Fabrication of Al5083/B4C surface composite by friction stir processing and its tribological characterization. *J. Mater. Res. Technol.* **2015**, *4*, 398–410. [CrossRef]
40. Srivastava, M.; Rathee, S.; Maheshwari, S.; Siddiquee, A.N. Influence of multiple-passes on microstructure and mechanical properties of Al-Mg/SiC surface composites fabricated via underwater friction stir processing. *Mater. Res. Express* **2018**, *5*, 066511. [CrossRef]
41. Srivastava, M.; Rathee, S.; Siddiquee, A.N.; Maheshwari, S. Investigation on the effects of silicon carbide and cooling medium during multi-pass FSP of Al-Mg/SiC surface composites. *Silicon* **2019**, *11*, 2149–2157. [CrossRef]
42. Li, Q.; Huang, G.; Cao, Y.; Zhang, C.; He, J.; Jiang, H.; Lin, L.; Liu, Q. Microstructure refinement, strengthening and ductilization mechanisms in Al–Mg–Mn–Er–Zr alloy with high Mn content by friction stir processing. *Mater. Charact.* **2022**, *189*, 111939. [CrossRef]
43. Amra, M.; Ranjbar, K.; Hosseini, S.A. Microstructure and wear performance of Al5083/CeO2/SiC mono and hybrid surface composites fabricated by friction stir processing. *Trans. Nonferrous Met. Soc. China* **2018**, *28*, 866–878. [CrossRef]
44. Faraji, G.; Dastani, O.; Mousavi, S.A. Effect of process parameters on microstructure and micro-hardness of AZ91/Al 2 O 3 surface composite produced by FSP. *J. Mater. Eng. Perform.* **2011**, *20*, 1583–1590. [CrossRef]
45. Bharathikanna, R.; Elatharasan, G. An investigation on microstructures and mechanical properties of AA1050 in friction stir processing technique. *Adv. Nat. Appl. Sci.* **2017**, *11*, 316–322.
46. Huang, G.; Wu, J.; Hou, W.; Shen, Y. Microstructure, mechanical properties and strengthening mechanism of titanium particle reinforced aluminum matrix composites produced by submerged friction stir processing. *Mater. Sci. Eng. A* **2018**, *734*, 353–363. [CrossRef]
47. Agha Amini Fashami, H.; Bani Mostafa Arab, N.; Hoseinpour Gollo, M.; Nami, B. Numerical and experimental investigation of defects formation during friction stir processing on AZ91. *SN Appl. Sci.* **2021**, *3*, 1–13. [CrossRef]
48. Habibnia, M.; Shakeri, M.; Nourouzi, S.; Givi, M.B. Microstructural and mechanical properties of friction stir welded 5050 Al alloy and 304 stainless steel plates. *Int. J. Adv. Manuf. Technol.* **2015**, *76*, 819–829. [CrossRef]

49. Zandsalimi, S.; Heidarzadeh, A.; Saeid, T. Dissimilar friction-stir welding of 430 stainless steel and 6061 aluminum alloy: Microstructure and mechanical properties of the joints. *Proc. Inst. Mech. Eng. Part L J. Mater. Des. Appl.* **2019**, *233*, 1791–1801. [CrossRef]
50. Akbari, M.; Ezzati, M.; Asadi, P. Investigation of the effect of tool probe profile on reinforced particles distribution using experimental and CEL approaches. *Int. J. Lightweight Mater. Manuf.* **2022**, *5*, 213–223. [CrossRef]
51. Hamilton, C.; Kopyściański, M.; Senkov, O.; Dymek, S. A coupled thermal/material flow model of friction stir welding applied to Sc-modified aluminum alloys. *Metall. Mater. Trans. A* **2013**, *44*, 1730–1740. [CrossRef]
52. Hamilton, C.; Węglowski, M.S.; Dymek, S. A simulation of friction-stir processing for temperature and material flow. *Metall. Mater. Trans. B* **2015**, *46*, 1409–1418. [CrossRef]
53. Khan, N.Z.; Siddiquee, A.N.; Khan, Z.A.; Shihab, S.K. Investigations on tunneling and kissing bond defects in FSW joints for dissimilar aluminum alloys. *J. Alloys Compd.* **2015**, *648*, 360–367. [CrossRef]
54. Ahmadkhaniha, D.; Sohi, M.H.; Zarei-Hanzaki, A.; Bayazid, S.M.; Saba, M. Taguchi optimization of process parameters in friction stir processing of pure Mg. *J. Magnes. Alloys* **2015**, *3*, 168–172. [CrossRef]
55. Roy, R.K. *A Primer on the Taguchi Method*; Society of manufacturing engineers: Southfield, MI, USA, 2010.
56. Jain, V.K.; Yadav, M.K.; Siddiquee, A.N.; Khan, Z.A. Optimization of friction stir processing parameters for enhanced microhardness of AA5083/Al-Fe in-situ composites via Taguchi technique. *Mater. Sci. Eng. Appl.* **2021**, *1*, 55–61. [CrossRef]
57. Kolli, M.; Naresh, D.S.; Devaraju, A.; Satyanarayana, K. Investigation of mechanical properties in friction stir processing parameters of Cu-TiB2 composite using Taguchi approach. *Int. J. Interact. Des. Manuf.* **2023**, 1–12. [CrossRef]
58. Muthukrishnan, N.; Davim, J.P. Optimization of machining parameters of Al/SiC-MMC with ANOVA and ANN analysis. *J. Mater. Process. Technol.* **2009**, *209*, 225–232. [CrossRef]
59. Vigneshkumar, M.; Padmanaban, G.; Balasubramanian, V. Influence of tool tilt angle on the formation of friction stir processing zone in cast magnesium alloy ZK60/SiCp surface composites. *Metallogr. Microstruct. Anal.* **2019**, *8*, 58–66. [CrossRef]
60. Chanakyan, C.; Sivasankar, S.; Meignanamoorthy, M.; Ravichandran, M.; Mohanavel, V.; Alfarraj, S.; Almoallim, H.S.; Manikandan, V.; Isaac JoshuaRamesh Lalvani, J. Optimization of FSP process parameters on AA5052 employing the S/N ratio and ANOVA method. *Adv. Mater. Sci. Eng.* **2021**, *2021*, 6450251. [CrossRef]
61. Syed, K.; Ali, M.A.; Reddy, K.P.; Rao, B.N. Analyzing the Influence of Tool Profile on Friction Stir Process with Taguchi Optimization and Tungsten Nano Powder. *Int. J. Veh. Struct. Syst.* **2023**, *15*, 802–807.
62. Butola, R.; Ranganath, M.S.; Murtaza, Q. Fabrication and optimization of AA7075 matrix surface composites using Taguchi technique via friction stir processing (FSP). *Eng. Res. Express* **2019**, *1*, 025015. [CrossRef]
63. Muribwathoho, O.; Msomi, V.; Mabuwa, S. An Analysis Comparing the Taguchi Method for Optimizing the Process Parameters of AA5083/Silicon Carbide and AA5083/Coal Composites That Are Fabricated via Friction Stir Processing. *Appl. Sci.* **2024**, *14*, 9616. [CrossRef]